

# V-ATPase Subunit ATP6AP1 (Ac45) Regulates Osteoclast Differentiation, Extracellular Acidification, Lysosomal Trafficking, and Protease Exocytosis in Osteoclast-Mediated Bone Resorption

De-Qin Yang,<sup>1,2,3,4\*</sup> Shengmei Feng,<sup>1,2,5\*</sup> Wei Chen,<sup>1,2</sup> Haibo Zhao,<sup>6</sup> Christie Paulson,<sup>1,2</sup> and Yi-Ping Li<sup>1,2</sup>

<sup>1</sup>Department of Pathology, University of Alabama at Birmingham, Birmingham, AL, USA

<sup>2</sup>Department of Cytokine Biology, The Forsyth Institute, Boston, MA, USA

<sup>3</sup>Stomatological Hospital of Zunyi Medical College, Zunyi, Guizhou Province, People's Republic of China

<sup>4</sup>The Affiliated Hospital of Stomatology, Chongqing Medical University, Chongqing, People's Republic of China

<sup>5</sup>Shanghai Key Laboratory for Prevention and Treatment of Bone and Joint Diseases with Integrated Chinese-Western Medicine, Shanghai Institute of Trauma and Orthopaedics, Ruijin Hospital, School of Medicine, Shanghai Jiao-Tong University, Shanghai, People's Republic of China

<sup>6</sup>Department of Internal Medicine, College of Medicine, University of Arkansas for Medical Sciences, Little Rock, AR, USA

## ABSTRACT

Lysosomal trafficking and protease exocytosis in osteoclasts are essential for ruffled border formation and bone resorption. Yet the mechanism underlying lysosomal trafficking and the related process of exocytosis remains largely unknown. We found ATP6ap1 (Ac45), an accessory subunit of vacuolar-type H<sup>+</sup>-ATPases (V-ATPases), to be highly induced by receptor activator for nuclear factor kappa B ligand (RANKL) in osteoclast differentiation. Ac45 knockdown osteoclasts formed normal actin rings, but had severely impaired extracellular acidification and bone resorption. Ac45 knockdown significantly reduced osteoclast formation. The decrease in the number of osteoclasts does not result from abnormal apoptosis; rather, it results from decreased osteoclast precursor cell proliferation and fusion, which may be partially due to the downregulation of extracellular signal-regulated kinase (ERK) phosphorylation and FBJ osteosarcoma oncogene (c-fos), nuclear factor of activated T-cells, cytoplasmic 1 (NFATc1), and "transmembrane 7 superfamily member 4" (Tm7sf4) expression. Notably, Ac45 knockdown osteoclasts exhibited impaired lysosomal trafficking and exocytosis, as indicated by the absence of lysosomal trafficking to the ruffled border and a lack of cathepsin K exocytosis into the resorption lacuna. Our data revealed that the impaired exocytosis is specifically due to Ac45 deficiency, and not the general consequence of a defective V-ATPase. Together, our results demonstrate the essential role of Ac45 in osteoclast-mediated extracellular acidification and protease exocytosis, as well as the ability of Ac45 to guide lysosomal intracellular trafficking to the ruffled border, potentially through its interaction with the small guanosine-5'-triphosphatase (GTPase) Rab7. Our work indicates that Ac45 may be a novel therapeutic target for osteolytic disease. © 2012 American Society for Bone and Mineral Research.

**KEY WORDS:** V-ATPase SUBUNIT ATP6AP1 (Ac45); OSTEOCLAST; LYSOSOMAL TRAFFICKING; PROTEASE EXOCYTOSIS; BONE RESORPTION

## Introduction

Osteoclasts are multinucleated cells of bone marrow lineage that are responsible for bone resorption through degradation of the organic and inorganic bone matrix. Osteoclasts exert a profound impact on skeletal metabolism and dynamic balance: either too much or too little osteoclast activity could lead to bone disorders, such as osteoporosis or osteopetrosis, respectively.

Osteoclasts resorb bone by attaching to the bone surface and forming a resorption lacuna surrounded by a ruffled border, and then secreting protons into the extracellular compartment.<sup>(1)</sup> The ruffled border is the "resorptive organelle" of the osteoclast and is formed by the polarized targeting and fusion of acidified vesicles with the plasma membrane through intracellular vesicular trafficking.<sup>(2-4)</sup> Because vesicular trafficking and the related mechanism of exocytosis are key to osteoclastic bone

Received in original form July 15, 2011; revised form March 14, 2012; accepted March 26, 2012. Published online March 29, 2012.

Address correspondence to: Yi-Ping Li, PhD, Department of Pathology, University of Alabama at Birmingham, SHEL 810, 1825 University Blvd, Birmingham AL 35294-2182, USA. E-mail: ypli@uab.edu

Additional Supporting Information may be found in the online version of this article.

\*D-QY and SF contributed equally to this work.

Journal of Bone and Mineral Research, Vol. 27, No. 8, August 2012, pp 1695-1707

DOI: 10.1002/jbmr.1623

© 2012 American Society for Bone and Mineral Research

resorption, there is a great need to better understand these mechanisms.<sup>(5)</sup>

Vacuolar-type H<sup>+</sup>-ATPases (V-ATPases) are primarily responsible for proton secretion and intracellular vesicle acidification. It has been suggested that V-ATPases are involved in a wide variety of physiological processes, including endocytosis, exocytosis, intracellular membrane trafficking, membrane fusion, and cell–cell fusion.<sup>(6–9)</sup> Understanding the molecular and cellular mechanisms by which V-ATPases regulate endocytosis, exocytosis, and intracellular trafficking in bone-resorbing osteoclasts will likely facilitate the development of novel and selective inhibitors for the treatment of lytic bone disorders.

ATP6ap1 (Ac45), an accessory subunit of the V-ATPase complex, is a type I transmembrane protein associated with the V-ATPase membrane domain (V0). Ac45 knockout results in early embryonic lethality, indicating that Ac45 is essential to embryonic development.<sup>(10)</sup> Louagie and colleagues<sup>(11)</sup> demonstrated that impaired processing of Ac45 may be responsible for disturbed intragranular acidification in the endocrine pancreas. Jansen and colleagues<sup>(12)</sup> reported that Ac45 was intrinsically capable of mediating endocytosis of a cell-surface protein in CV-1 kidney fibroblasts, indicating that the cytoplasmic tail of Ac45 contains an internalization signal for endocytosis. Recently, overexpression of an Ac45 cytoplasmic terminus deletion mutant in RAW264.7 cells resulted in a dramatic reduction in osteoclast-mediated bone resorption and alterations in the binding proximity of Ac45 with the V-ATPase V0 domain subunits  $\alpha 3$ ,  $c'$ , and  $d$ .<sup>(13)</sup> Another study pointed toward the physiologic importance of the entire Ac45 protein by revealing that the intact N-linked glycosylated Ac45 is cleaved into a C-terminal (42 ± 44 kDa) fragment and a previously unreported N-terminal (~22 kDa) fragment in the endoplasmic reticulum or cis-Golgi (where activation of the V-ATPase is necessary).<sup>(14)</sup> These studies demonstrate that Ac45 has diverse roles in different cells and stages of development. Numerous critical questions remain unanswered related to whether or not Ac45 plays an important role in osteoclast-mediated extracellular acidification, exocytosis in osteoclasts, or intracellular lysosomal trafficking to the ruffled border. The mechanism underlying Ac45's ability to guide lysosomes to the ruffled border also remains unknown. We began to address these critical questions by investigating the role of Ac45 in osteoclasts. Previous studies led us to hypothesize that Ac45 may regulate vesicular intracellular trafficking and protease exocytosis in resorbing osteoclasts. We determined that osteoclasts have a high expression level of Ac45 after receptor activator for nuclear factor kappa B ligand (RANKL) induction. Because there are likely distinct functional differences between the intact and truncated Ac45 protein, we used lentivirus-mediated RNA interference (RNAi) silencing to knockdown Ac45 gene expression and perform a loss-of-function study on the Ac45 protein that would reveal features of its physiological role. We revealed that Ac45 affects osteoclast-mediated acidification and bone resorption through its important roles in the regulation of lysosomal trafficking and protease exocytosis, as well as its role in osteoclast differentiation and cell fusion. We also revealed that lysosomal trafficking, osteoclast differentiation, and osteoclast fusion may be regulated through Ac45's involvement in the Rab7, extracellular signal-regulated

kinase (ERK)/nuclear factor of activated T-cells, cytoplasmic 1 (NFATc1)/FBJ osteosarcoma oncogene (*c-fos*), and “transmembrane 7 superfamily member 4” (Tm7sf4) signaling pathways, respectively. These findings provide essential insight to long-standing cell biology questions regarding the mechanism underlying lysosomal trafficking and exocytosis, processes that are indispensable for proper osteoclastic bone resorption.

## Materials and Methods

### Constructs and Western blotting

We designed five short hairpin RNA (shRNA) specifically targeting the mRNA of mouse Ac45 (NM\_018794) using The RNAi Consortium (TRC) (<http://www.broadinstitute.org/rnai/public>) with the sense strand sequences of 5'-<sup>1745</sup>CCTTGCTGTTA-CCTTGCTGTTTATAGTGCTT<sup>1765</sup>-3'(ac45s1), 5'-<sup>1344</sup>GCATGAT-ACTCAGCCTAAA<sup>1364</sup>-3'(ac45s2), 5'-<sup>1075</sup>GCCCATTTCAATGTTCC-CAA<sup>1095</sup>-3'(ac45s3), 5'-<sup>274</sup>CGTAATGTACTGCTTCTA<sup>294</sup>-3'(ac45s4), and 5'-<sup>844</sup>GCATACAAAGACGAGTGGA<sup>864</sup>-3'(ac45s5). The negative control small interfering RNA (siRNA) targeting green fluorescent protein (GFP) is 5'-ACAACAGCCACAACGTCTATA-3'. The siRNA targeting ATP6v1e1 (NM\_007510.2) as a control is 5'-<sup>806</sup>GCTTCTCTTTCTGTTCTAAT<sup>826</sup>-3'. The shRNA oligonucleotides were annealed and ligated into the AgeI-EcoRI cloning site of the pLKO.1 vector, which carries the puromycin-resistance gene and drives shRNA expression from a human U6 promoter. SDS-PAGE and Western blot analysis were carried out as our laboratory described.<sup>(15,16)</sup>

### Confocal microscopy and 3D reconstruction for lysosomal intracellular trafficking and exocytosis of cathepsin K in osteoclasts

Confocal microscopy and 3D reconstruction were performed in the Optical Image Office of Harvard Neurodiscovery Center (Boston, MA, USA) and the University of Alabama at Birmingham (UAB) High Resolution Imaging Facility (Birmingham, AL, USA) to observe the intracellular trafficking of lysosomal marker lamp-1, V-ATPases, and the exocytosis of cathepsin K. For observation of lysosomal intracellular trafficking in nonresorbing (nonpolarized) osteoclasts, mouse bone marrow (MBM) was cultured on glass slices. For observation of lysosomal intracellular trafficking in resorbing (polarized) osteoclasts, MBM was cultured on dentin slices or bone slices. To localize the V-ATPase, we used three different antibodies (1:75): anti-ATP6v0a3, anti-ATP6v1b2, and anti-ATP6v1c1. Fluorescent antibody distribution was monitored with a Zeiss LSM 510 confocal laser-scanning microscope (Carl Zeiss, Oberkochen, Germany) using standard filter settings and sequential scanning to avoid crosstalk. For the exocytosis assay, cathepsin K antibodies (1:100), and 2 U/mL rhodamine phalloidin were used to co-stain cathepsin K and the actin ring of osteoclasts cultured on dentin slices. For both assays, MBM cells were isolated and cultured in 24-well plates in  $\alpha$  modified essential medium ( $\alpha$ -MEM) with 10 ng/mL macrophage colony-stimulating factor (M-CSF) and 10 ng/mL RANKL for 48 hours and then cells were transduced with lentivirus. Untransduced cells (mock) and transduced cells were cultured with M-CSF/RANKL for a total of 5 days before analysis. The thickness of the optical

section was set to 1  $\mu\text{m}$  for the z-stack scan. In some images, the maximum projection image was generated to allow the visualization of the area just above the bone surface to the bottom of the pit. For 3D reconstruction, the optical thickness of the x-y sections was set to 0.5  $\mu\text{m}$  and sections were collected from the top of the cell to the bottom of the pit. The sections were then added together with Imaris software (Bitplane, Zürich, Switzerland) and displayed as x-z and y-z sections of the whole cell. Experiments were repeated three times.

### Immunofluorescence colocalization

MBM was grown on bone slices and induced by RANKL and M-CSF for 5 days. The cells were then fixed with 2% formaldehyde in PBS for 20 minutes, washed with PBS three times, incubated in 0.2% Triton X-100 for 15 minutes, and blocked for 1 hour with 10% normal goat serum in PBS. Additionally, cells were incubated in the primary antibodies (1:50), diluted in 1% normal serum in PBS overnight at 4°C, washed three times with PBS for 5 minutes, and incubated with either secondary antibody goat-anti-rabbit-fluorescein isothiocyanate (FITC) (1:50), goat-anti-rabbit-Texas Red (TR) (1:50), or with goat-anti-mouse-TR (1:50) for 1 hour. Cells were then washed with PBS and mounted with anti-fade mounting medium (gift from Dr. Shi-liang Ma). Observations were performed by fluorescence in a Zeiss LSM 510 confocal laser-scanning microscope (Carl Zeiss). (Please see Supplemental Materials and Methods for additional details.)

## Results

### Ac45 was highly expressed in mouse osteoclasts

To determine if Ac45, an accessory subunit of the V-ATPase, has an important role and function in osteoclasts, we first analyzed expression profiles of the Ac45 gene and protein in osteoclasts. Using microarray analysis as our laboratory and others have described,<sup>(15–17)</sup> we found that the mRNA expression level of Ac45 was induced about 3.5-fold higher in mature osteoclasts [MBM induced by M-CSF and RANKL for 5 days] than in monocytes (MBM induced by M-CSF alone for 5 days) (Fig. 1A). We used Western blot analysis to detect Ac45 protein expression (Fig. 1B) and found that the protein level of Ac45 continued to increase during osteoclast differentiation and maturation (normalized to the  $\beta$ -actin level; Fig. 1C). After 120 hours of RANKL and M-CSF induction, Ac45 protein expression was approximately 10-fold higher than at the 24-hour time point. These results indicated that Ac45 is much more highly expressed in osteoclasts compared to monocytes and that it can be induced by RANKL and M-CSF during osteoclast differentiation, suggesting that Ac45 may be of particular importance in mature osteoclasts.

### Ac45 expression was effectively depleted by lentivirus siRNA in osteoclasts

To accurately determine the effect of the loss-of-function of Ac45, we prepared five lentiviral constructs, which encode siRNAs that target Ac45. Through Western blot analysis, it was demonstrated that two of the five siRNAs (ac45s1 and ac45s2)

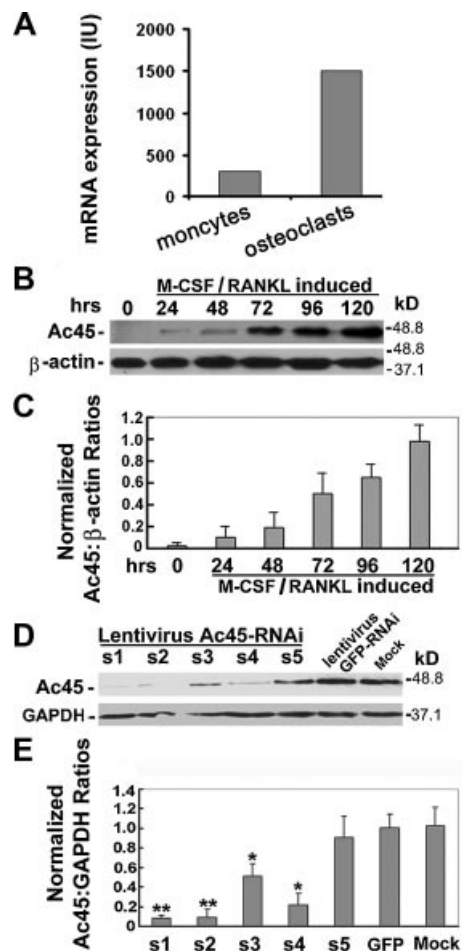


**Fig. 1.** Expression of Ac45 in osteoclasts and its effective depletion by lentiviral siRNA. (A) Microarray data of expression levels of Ac45 in monocytes and osteoclasts. IU = intensity units. (B) Western blot analysis of the time-course of Ac45 protein expression in MBM induced by M-CSF and RANKL. (C) The protein levels on time-course blot were analyzed and quantified with the NIH ImageJ software. The values shown represent ratios of Ac45 to  $\beta$ -actin protein levels that have been normalized ( $n = 3$ ). (D) Western blot verified Ac45 knockdown effect of 5 siRNAs by lentivirus-mediated transduction. GAPDH was used as a protein loading control and Lentivirus-GFP-RNAi as a transduction efficiency control. (E) The protein levels on blot were analyzed and quantified with the NIH ImageJ software. The values shown represent ratios of Ac45 to GAPDH protein levels that have been normalized ( $n = 3$ ). \* $p < 0.05$ , \*\* $p < 0.01$  compared with that of Lentivirus-GFP-RNAi treated cells.

had the ability to deplete about 90% of the expression of Ac45 in osteoclasts (Fig. 1D, E) in comparison to untransduced osteoclasts (mock) and to osteoclasts treated with siRNA targeting GFP. Therefore, we used the lentivirus packaged with pLCo.1-ac45s1 and pLCo.1-ac45s2 [named Lentivirus-Ac45-RNAi(s1) and Lentivirus-Ac45-RNAi(s2) respectively] to transduce osteoclasts for different functional assays. We also used the lentivirus packaged with pLCo.1-GFP (Lentivirus-GFP-RNAi) as an internal control. Lentiviral transduction itself did not cause any change in Ac45 expression since control osteoclasts transduced with Lentivirus-GFP-RNAi showed similar protein levels as mock cells (Fig. 1D, E). These results indicate an effective and specific depletion of Ac45 by siRNA in primary cultured osteoclasts.

## Knockdown of Ac45 reduced the formation of multinucleated osteoclasts

We determined through Western blot that Ac45 expression in osteoclasts was significantly knocked down by Lentivirus-Ac45-RNAi(s1) compared to osteoclasts treated with Lentivirus-GFP-RNAi (Fig. 2A, B). Transduction efficiency of Lentivirus-Ac45-RNAi(s1)

and Lentivirus-Ac45-RNAi(s2), which carried 10% reporter GFP DNA, was confirmed through GFP expression in almost all osteoclasts compared to the fluorescence expressed in osteoclasts transduced by Lenti-pLB that carried 100% reporter GFP DNA (Fig. 2C) as our laboratory described.<sup>(15)</sup> Compared to the control cells, there were fewer tartrate-resistant acid phosphatase (TRAP)-positive multinucleated osteoclasts (MNCs) (with

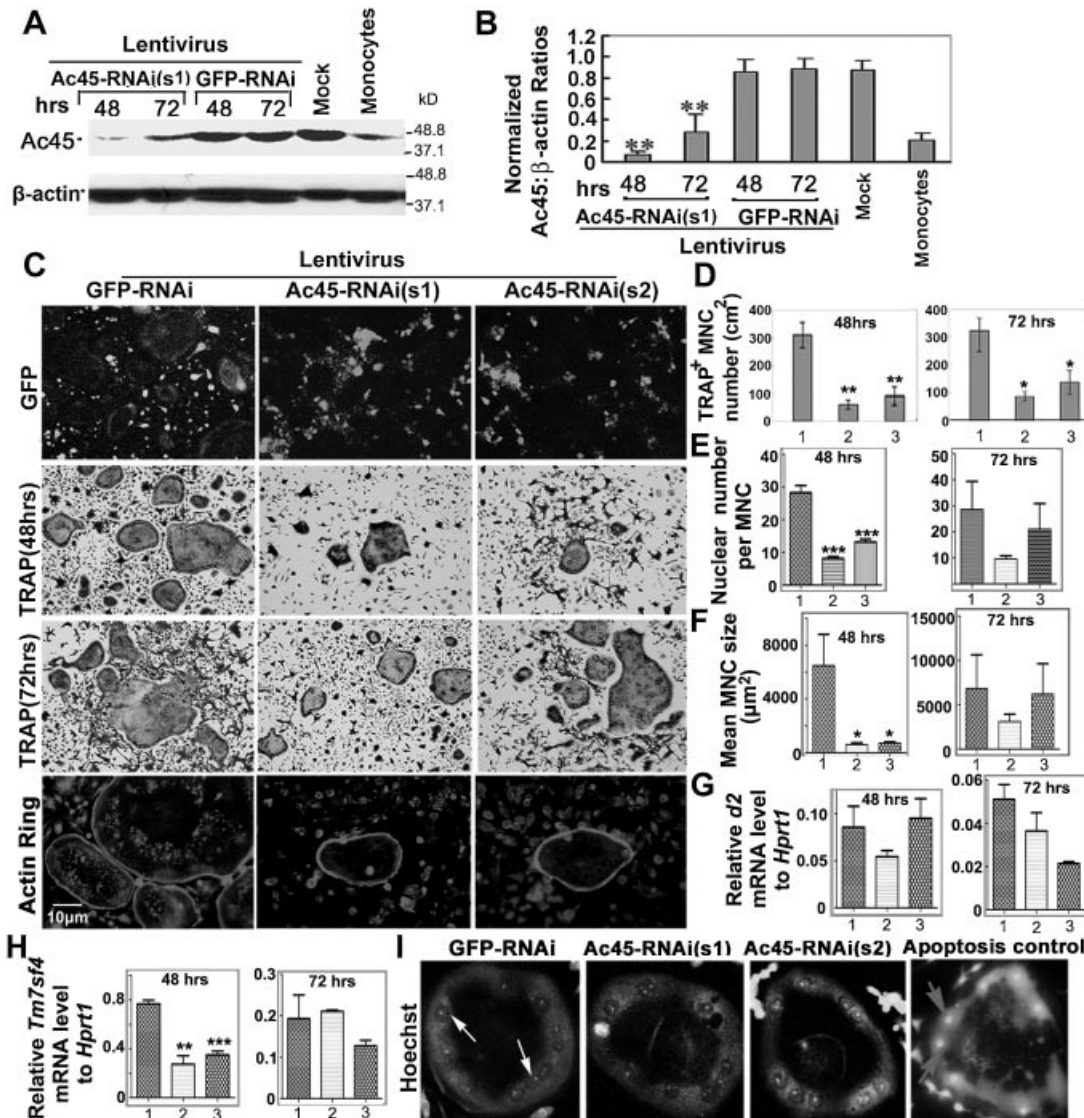


**Fig. 2.** Lentivirus-mediated knockdown of Ac45 reduced the formation of multinucleated osteoclasts, but it did not impair actin rings formation. (A) Western blot of Ac45 protein expression in mock cells and monocytes, as well as in osteoclasts transduced with Lentivirus-Ac45-RNAi (s1) and Lentivirus-GFP-RNAi after 48 or 72 hours of M-CSF/RANKL induction.  $\beta$ -actin was used as a protein loading control. (B) The protein levels on blot were analyzed and quantified with the NIH ImageJ software. The values shown represent ratios of Ac45 to  $\beta$ -actin protein levels that have been normalized ( $n = 3$ ). (C) Various assays performed on osteoclasts transduced with Lentivirus-GFP-RNAi, Lentivirus-Ac45-RNAi(s1), or Lentivirus-Ac45-RNAi(s2). Row 1: Verification of lentivirus transduction and siRNA expression through GFP reporter gene expression. Row 2 and 3: TRAP staining of osteoclasts transduced after 48 or 72 hours of M-CSF/RANKL induction as indicated. Row 4: Immunostaining of F-actin podosomal belts with rhodamine phalloidin. The osteoclasts shown were representative of the data ( $n = 3$ ). (D) Quantification of TRAP-positive multinucleated cell (MNC) number ( $\geq 3$  nuclei) in rows 2 and 3 of C. All data are expressed as mean  $\pm$  SD ( $n = 5$ ). (E) Quantification of the number of nuclei per MNC in rows 2 and 3 of C. All data are expressed as mean  $\pm$  SD ( $n = 10$ ). (F) Quantification of MNC size in rows 2 and 3 of C. All data are expressed as mean  $\pm$  SD ( $n = 10$ ). (G) *d2* mRNA expression level relative to *Hprt1* ( $n = 3$ ). (H) *Tm7sf4* mRNA expression level relative to *Hprt1* ( $n = 3$ ). In D–H, column 1 is Lentivirus-GFP-RNAi, column 2 is Lentivirus-Ac45-RNAi(s1), and column 3 is Lentivirus-Ac45-RNAi(s2). (I) Apoptosis assay with Hoechst 33258 staining in osteoclasts 48 hours after M-CSF/RANKL induction. Compared to the positive apoptosis control (apoptosis induced by M-CSF/RANKL starvation for 12 hours), apoptosis does not occur as a result of Ac45 depletion. Gray arrows indicate apoptotic nuclei and white arrows indicate normal nuclei. \* $p < 0.05$ , \*\* $p < 0.01$ , and \*\*\* $p < 0.001$  compared with that of Lentivirus-GFPi-treated cells at the same time points of transduction.

≥3 nuclei) in groups depleted of *Ac45* at the 48-hour and 72-hour time points (Fig. 2C, D), even though all groups were cultured with M-CSF/RANKL for a total of 5 days. Compared to the control group, the nuclei number per MNC and the average MNC size was significantly reduced in the group depleted of *Ac45* at the 48-hour time point, but not in the group depleted of *Ac45* at the 72-hour time point (Fig. 2E, F). Therefore, we checked the expression of fusion genes *Tm7sf4* and *d2*<sup>(18,19)</sup> to determine if *Ac45* has a role in osteoclast fusion. Interestingly, we found that *Tm7sf4* mRNA expression significantly decreased in groups depleted of *Ac45* at the 48-hour time point but not in groups depleted of *Ac45* at the 72-hour time point. Expression of *d2* was not significantly changed when *Ac45* was depleted at 48 or 72 hours (Fig. 2G, H). Hence, *Ac45* may also be important for the development of mature multinucleated osteoclasts.

### Ac45-depleted multinucleated osteoclasts formed normal filamentous actin rings and did not undergo apoptosis

To investigate if *Ac45*-depleted osteoclasts fail to form normal actin rings, which are formed during osteoclast maturation,<sup>(20)</sup> we used phalloidin staining for filamentous actin (F-actin). Although *Ac45* deficiency reduces the number of multinucleated osteoclasts, our results indicate that it does not affect the formation of F-actin podosomal belts in those multinucleated osteoclasts that do develop (Fig. 2C). To elucidate if cell apoptosis is the pathway by which depletion of *Ac45* impairs formation of multinucleated osteoclasts, we performed an apoptosis assay with Hoechst 33258 staining. Compared with the apoptosis control group, the nuclei of osteoclasts transduced with GFP-RNAi, Lentivirus-*Ac45*-RNAi(s1), and Lentivirus-*Ac45*-RNAi(s2) did not show the obvious chromatin condensation and/or nuclear fragmentation associated with apoptosis (Fig. 2I). Therefore, it is unlikely that *Ac45* influences the development of mature osteoclasts through cell apoptosis.

### Depletion of *Ac45* impaired extracellular acidification and decreased osteoclastic bone resorption

Because actin rings are intact in the multinucleated osteoclasts that form after *Ac45* knockdown at the 48-hour and 72-hour time points, it is important to clarify whether these osteoclasts are also capable of normal extracellular acidification and bone resorption. We measured the acidification activity by vital staining of osteoclasts with acridine orange.<sup>(21)</sup> Lentivirus-*Ac45*-RNAi(s1)- and Lentivirus-*Ac45*-RNAi(s2)-transduced osteoclasts displayed little orange-red staining (indicates active production of H<sup>+</sup> and extracellular acidification) compared to mock and Lentivirus-GFP-RNAi osteoclasts. This indicates a severe block of acidification activity due to the knockdown of *Ac45*. Since ATP6v1e1 is a core subunit of the osteoclast V-ATPase and not an accessory subunit like *Ac45*, it is expected that its depletion will impair extracellular acidification. Thus, we transduced an additional group of cells with Lentivirus-ATP6v1e1-RNAi as a control. The Lentivirus-ATP6v1e1-RNAi effectively and specifically depleted about 90% of the expression of ATP6v1e1 in osteoclasts, compared with the Lentivirus-GFP-RNAi group (data not shown). As expected, osteoclasts transduced with Lentivirus-ATP6v1e1-RNAi also had little orange-red staining (Fig. 3A). This result

promotes us to further determine if impaired extracellular acidification is the result of general damage to the V-ATPase. So, we used confocal microscopy to observe Atp6v0a3 (a3) and Atp6v1c1 (C1) colocalization to determine if *Ac45* knockdown impaired assembly of the V-ATPase complex as described.<sup>(22)</sup> We found that *Ac45* knockdown has no effect on osteoclast V-ATPase assembly because a3 colocalized with C1 as in the control osteoclasts. Importantly, we found that a3 and C1 colocalized mostly on the plasma membrane of control osteoclasts and mostly in the cytoplasm of the *Ac45*-knockdown osteoclasts (Fig. 3B). This result suggests that *Ac45* knockdown has no effect on V-ATPase assembly and that the decrease in osteoclast extracellular acidification when *Ac45* is knocked down may be partially due to impaired V-ATPase trafficking to the plasma membrane.

We also assessed the formation of resorption pits on bovine cortical bone slices by mock and Lentivirus-GFP-RNAi control osteoclasts and by osteoclasts transduced with Lentivirus-*Ac45*-RNAi(s1) or Lentivirus-*Ac45*-RNAi(s2) after 48 or 72 hours of M-CSF/RANKL induction. All cells were cultured with M-CSF/RANKL for a total of 5 days. We seeded the same number of MBM cells on each bone slice (Fig. 3C–E). Corresponding with our previous finding that *Ac45* knockdown inhibits MNCs formation, there were less MNCs in the *Ac45* knockdown group (Fig. 3F). Our ELISA assay revealed that there was a significant reduction in the cross-linked C-telopeptide (CTX) concentration in *Ac45*-knockdown osteoclast culture media compared to the control osteoclast media (Fig. 3G). In addition, scanning electron microscopy analysis of the bone slices indicated that *Ac45*-depleted osteoclasts had a dramatic reduction in bone resorption (2%–7% resorbed area per mm<sup>2</sup>) compared to control cells (approximately 60% resorbed area) (Fig. 3H, I). Taken together, these results suggest that *Ac45* is essential for the extracellular acidification and bone resorption of osteoclasts.

### Depletion of *Ac45* resulted in defective lysosomal trafficking and sorting toward the ruffled border

A key step for extracellular acidification and bone resorption is the insertion of V-ATPases into the lysosomal membrane and their recruitment to the ruffled border. In Fig. 3B, we found that *Ac45* knockdown may block V-ATPase trafficking to the plasma membrane but that it does not affect V-ATPase assembly. Accordingly, we examined if *Ac45* knockdown in osteoclasts blocks lysosomal trafficking. It has been reported that in osteoclasts, V-ATPases with the a3 isoform were immunohemically colocalized with lysosome marker lamp2 and detected in acidic organelles.<sup>(23)</sup> Furthermore, V-ATPases with the a3 isoform localized in late endosomes/lysosomes that are transported to the cell periphery during differentiation and finally assembled into the plasma membrane of mature osteoclasts.<sup>(23)</sup> Consequently, we first used a3 localization to indirectly address the role of *Ac45* in lysosomal trafficking. We also used Atp6v1b2 (B2) and Atp6v1c1 (C1) subunits to further indicate the effect of *Ac45* on lysosomal trafficking because B2<sup>(24)</sup> and C1<sup>(15)</sup> are also specific subunits in the osteoclast plasma V-ATPase. In both nonresorptive cells on glass slices (Fig. 4IA–I) and resorptive cells on dentin slices (Fig. 4IU–U), the V-ATPase diffused throughout the

cytoplasm in the Ac45-depleted group (Fig. 4IG–I, P–R, U) compared to the mock (Fig. 4IA–C, J–L, S) and Lentivirus-GFP-RNAi (Fig. 4ID–F, M–O, T) control groups in which V-ATPase was localized to the ruffled border. The z-axis view in the 3D system provides a view of the diffusion of the V-ATPase throughout

osteoclast cytoplasm in Ac45-depleted cells (Fig. 4IPz–Rz), which is contrasted by the precise targeting of the V-ATPase to the bone surface in control cells (Fig. 4IJz–Oz). Notably, the 3D reconstruction of the bone surface shows that the Ac45-depleted cells, unlike the control (Fig. 4IT) and mock cells (Fig. 4IS),

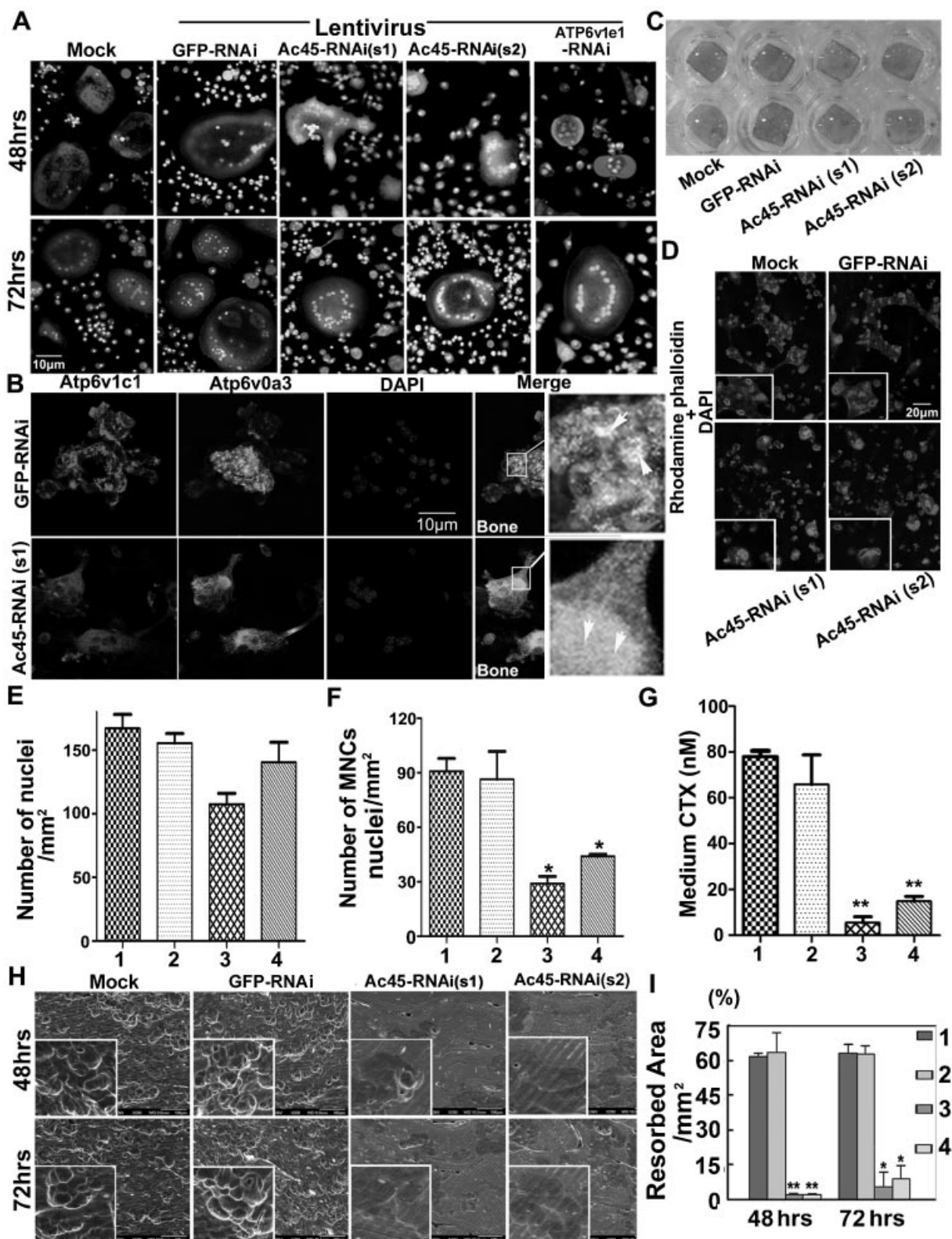


Fig. 3.

appeared to maintain a nonpolarized status (Fig. 4IU). These findings indirectly indicate that lysosomes lost their targeted trafficking ability when Ac45 was knocked down. To further confirm these findings, we used lysosome marker lamp-1, together with osteoclast-specific V-ATPase subunit a3, to directly determine if knockdown of ac45 impairs lysosomal trafficking in osteoclasts on bone slices. In mock and Lentivirus-GFP-RNAi control resorptive osteoclasts, both lamp-1 (red, Fig. 4IID, E) and a3 (green, Fig. 4IIA, B) were localized to the ruffled border within the resorption zone (Fig. 4IIA, B, D, E, white arrows). In contrast, both lamp-1 (red, Fig. 4IIF) and a3 (green, Fig. 4IIC) diffused throughout the cytoplasm in Ac45-depleted osteoclasts. The *xz* and *yz* views in the 3D system provide additional views of the diffusion of a3 and lamp-1 throughout the osteoclast cytoplasm in Ac45-depleted cells (Fig. 4IIL), which is contrasted by the precise targeting of a3 and lamp-1 to the bone surface in control cells (Fig. 4IIL, K, white arrows). Notably, a3 and lamp-1 are always associated, both in control osteoclasts (Fig. 4IIG, H, J, K, white arrows) and in ac45-depleted osteoclasts (Fig. 4IIL, L). Together, our data demonstrates that lysosomal trafficking to the ruffled border is lost in Ac45-depleted osteoclasts, which indicates that Ac45 has a role in regulating V-ATPase and lysosomal trafficking and sorting.

### Depletion of Ac45 impaired exocytosis of cathepsin K

To explore whether the exocytosis of cathepsin K (a protease involved in bone resorption) is also impaired by Ac45 depletion, we performed cathepsin K and actin ring co-staining in osteoclasts on bone slices. In mock (Fig. 5A–C) and Lentivirus-GFP-RNAi control (Fig. 5D–F) cells, large amounts of cathepsin K were exocytosed into the resorption lacunae circumscribed by actin rings. Cells treated with Lentivirus-Ac45-RNAi(s1) or Lentivirus-Ac45-RNAi(s2) formed actin rings (Fig. 5G, J); however, cathepsin K remained chiefly located in the cytoplasm (Fig. 5I, L) instead of accumulating within the actin ring and being exocytosed as in the mock and control cells (Fig. 5C, F). The *z*-axis view in the 3D system provides a better view of the exocytosis of cathepsin K in the extracellular resorptive compartment between the cell and surface of the dentin slice at the resorption pit site (Fig. 5Dz–Fz). This exocytosis of cathepsin K was totally blocked by Ac45 depletion, as shown by the absence of cathepsin K in the resorption lacunae (Fig. 5Jz–Lz). Osteoclasts were also transduced by Lentivirus-ATP6v1e1-RNAi in order to compare the function of Ac45 with that of a core V-ATPase subunit. Similar to mock and Lentivirus-GFP-RNAi groups, we

observed that osteoclasts transduced with Lentivirus-ATP6v1e1-RNAi had a higher concentration of cathepsin K within the actin ring than without (Fig. 5M–O). We further checked the cathepsin K protein level in osteoclast culture media and found that Ac45 knockdown significantly reduced cathepsin K secretion in the media (Fig. 5P–R). Together, these results demonstrate that cathepsin K can be produced in Ac45-depleted osteoclasts, but that its exocytosis toward resorption lacunae via the ruffled border is markedly inhibited.

### Ac45 interacts with small guanosine-5'-triphosphatase Rab7

It is known that Rab7, a small guanosine-5'-triphosphatase (GTPase), is involved in vesicular trafficking.<sup>(25)</sup> As an initial investigation of the relationship between Ac45 and Rab7 in the mechanism underlying extracellular acidification, lysosomal trafficking, and cathepsin K exocytosis, we performed an immunostaining analysis. We found that Ac45 colocalized with Rab7 in resorbing osteoclasts cultured on bone slices (Fig. 6A). In addition, a coimmunoprecipitation assay revealed that Ac45 directly interacted with Rab7, but not with Rac1 (Rac1 is important for regulation of the actin cytoskeleton<sup>(25)</sup>) (Fig. 6B). Furthermore, immunoprecipitation of the fusion protein FLAG-Rab7 with monoclonal anti-FLAG and Western blot analysis show that Ac45 was precipitated with both wild-type Rab7 and its active form RAB7Q67L (Fig. 6C). Osteoclasts that had been transduced with empty vectors and the total cell lysates (TCL) were used as controls. Our results suggest that Ac45 directly interacts with both the wild-type and the constitutively active forms of Rab7 and that Ac45 colocalizes with Rab7 in resorbing osteoclasts. Therefore, Ac45's role in extracellular acidification, lysosomal trafficking, and cathepsin K exocytosis may be through the Rab7 pathway.

### Knockdown of Ac45 reduced osteoclast differentiation, osteoclast precursor cell proliferation, and the expression of proteins that promote osteoclastogenesis

During our initial investigation of the role of Ac45 in osteoclast function, we noted that the formation of multinucleated osteoclasts was significantly inhibited (Fig. 2). In order to further clarify the role of Ac45 in the differentiation of mononuclear cells to mature osteoclasts, MBM cells were transduced with lentivirus after 12 or 24 hours of culture in  $\alpha$ -MEM with 10 ng/mL M-CSF and 10 ng/mL RANKL. After the transduced cells were cultured for an additional 4 to 5 days, we determined that Ac45-depleted

**Fig. 3.** Depletion of Ac45-impaired extracellular acidification, V-ATPase trafficking to the plasma membrane, and osteoclastic bone resorption. (A) Acridine orange staining of mock osteoclasts and osteoclasts transduced by Lentivirus-GFP-RNAi, Lentivirus-Ac45-RNAi(s1), Lentivirus-Ac45-RNAi(s2), and Lentivirus-ATP6v1e1-RNAi (as a control) after 48 or 72 hours of M-CSF/RANKL induction. (B) Atp6v1c1 and Atp6v0a3 immunofluorescence staining of osteoclasts as indicated, white arrows indicate colocalization of Atp6v1c1 and Atp6v0a3. (C) TRAP staining of bone discs with osteoclasts as indicated. (D) Rhodamine phalloidin and DAPI staining of osteoclasts on bone as indicated. (E) Quantification of nuclei per mm<sup>2</sup> in D (*n* = 5). (F) Quantification of MNCs' nuclei per mm<sup>2</sup> in D (*n* = 5). (G) ELISA assay of CTX concentration in osteoclast culture media as indicated. (H) Bone resorption pits on bovine cortical bone slices resulting from mock osteoclasts and osteoclasts transduced with Lentivirus-GFP-RNAi, Lentivirus-Ac45-RNAi(s1), and Lentivirus-Ac45-RNAi(s2) after 48 or 72 hours of M-CSF/RANKL induction. The bone slices were subjected to scanning electron microscopy analysis. White inset boxes: higher magnification view of the bone resorption pits. (I) Quantification of percentage of resorption area per mm<sup>2</sup> among the groups at different time points of transduction (*n* = 3). In E, F, G, and I, column 1 is mock, column 2 is Lentivirus-GFP-RNAi, column 3 is Lentivirus-Ac45-RNAi(s1), and column 4 is Lentivirus-Ac45-RNAi(s2). \**p* < 0.05, \*\**p* < 0.01 compared with that of Lentivirus-GFP-RNAi-treated cells. All results are mean  $\pm$  SD.



groups had a dramatic reduction in the number of TRAP<sup>+</sup> multinucleated osteoclasts compared to the control groups (Fig. 7A, B). However, differentiation of TRAP<sup>+</sup> mononuclear cells from MBM was not affected (Fig. 7A). This further demonstrates

that cell-cell fusion is severely impaired by Ac45 deficiency as in Fig. 2C–H. However, it is still unclear if Ac45 knockdown decreases the final number of osteoclasts by influencing osteoclast precursor cell proliferation and apoptosis. To address

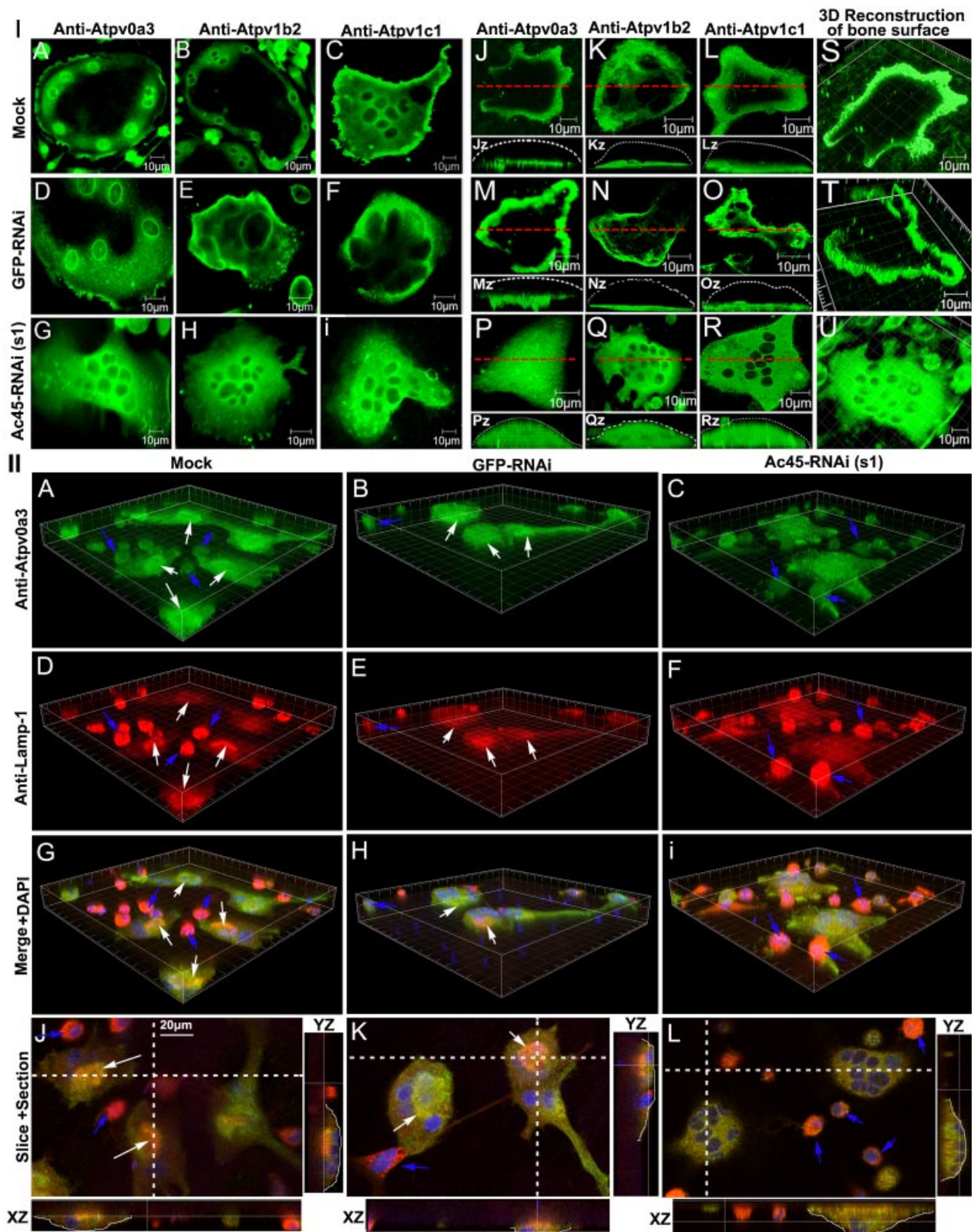


Fig. 4.



this question, monocytes were transduced at the 12-hour time point. After an additional 48 hours of induction with M-CSF, cells were incubated with bromodeoxyuridine (BrdU) for 2.5 hours or incubated with  $\alpha$ -MEM without fetal bovine serum (FBS) and M-CSF for 24 hours. We found that the Ac45-depleted group had a dramatic reduction in the ratio of BrdU-positive cells (Fig. 7C, D), but had no significant difference in the ratio of terminal deoxynucleotidyl transferase-mediated deoxyuridine triphosphate-biotin nick end labeling (TUNEL)-positive cells compared to the controls (Fig. 7E, F). To understand the mechanism of Ac45's role in osteoclastogenesis, we examined if Ac45 knockdown affects the ERK/c-fos/NFATc1 signaling pathway, which is known to be important for osteoclast differentiation.<sup>(26)</sup> Western blot revealed that protein expression of phosphorylated ERK (p-ERK), c-fos, and NFATc1 was significantly downregulated when Ac45 was knocked down at the 24-hour or 72-hour time point (Fig. 7G, H). Our findings indicate that Ac45 is involved in the ERK/c-fos/NFATc1 signaling pathway, thereby regulating osteoclast differentiation.

## Discussion

Our research on the Ac45 protein, a V-ATPase accessory subunit, demonstrated that Ac45 is highly expressed in osteoclasts and important for osteoclast precursor cell differentiation and fusion, but not for actin ring formation. Our results also showed that Ac45 is required for osteoclast-mediated extracellular acidification and bone resorption. In addition, Ac45 is important for intracellular trafficking and sorting of lysosomes to the ruffled border in osteoclasts and for the exocytosis of cathepsin K.

Surprisingly, knockdown of Ac45 after 48 or 72 hours of RANKL/M-CSF induction reduced the formation of multinucleated osteoclasts (Fig. 2C–F), which is similar to the recent report by Qin and colleagues.<sup>(27)</sup> The underlying mechanism did not involve apoptosis (Fig. 2I), but it did involve the downregulation of the fusion gene *Tm7sf4* (especially at the 48-hour transduction time point). Ac45 may have important functions related to osteoclastogenesis that remain to be further explored. Our results in Fig. 7 provided additional insight to the role of Ac45 in osteoclast differentiation. We found that Ac45 knockdown blocked osteoclast precursor cell proliferation, but had no effect on their apoptosis (Fig. 7C–F). During the process of osteoclastogenesis, RANKL activates TNF receptor-associated factor 6 (TRAF6), which leads to the activation of ERK through p-ERK.<sup>(28)</sup>

Sustained ERK activity induces c-fos expression and stabilization.<sup>(29)</sup> In turn, c-fos induces NFATc1, the major transcription factor of osteoclastogenesis.<sup>(26)</sup> The role of Ac45 in this signaling pathway is supported by our findings that Ac45 is important for the differentiation of TRAP<sup>+</sup> mononuclear cells to mature osteoclasts and for cell fusion (Figs. 2 and 7). Notably, protein expression of p-ERK, c-fos, and NFATc1 was downregulated by Ac45 knockdown (Fig. 7G, H), suggesting that Ac45 acts upstream of the ERK/c-fos/NFATc1 signaling pathway which regulates osteoclast differentiation.

Despite the inhibition of osteoclast differentiation resulting from Ac45 knockdown, a significant number of multinucleated osteoclasts are still present after Ac45 knockdown and allow for functional studies. Although these Ac45-depleted osteoclasts are capable of actin ring formation (Fig. 2C), they had little to no extracellular acidification activity (Fig. 3A), which may be due to impaired polarization of V-ATPases to the plasma membrane (Fig. 3B). Ac45-depleted osteoclasts also had severely impaired bone resorption (Fig. 3G–I). Confocal microscopy and 3D reconstruction indirectly revealed that unlike mock cells, osteoclasts transduced with Lentivirus-Ac45-RNAi(s2) do not form deep bone resorption pits (Fig. 5Ez, Kz). These results confirm and build on the findings of a previous study which reported that the cytoplasmic terminus of Ac45 may play an important role in osteoclastic bone resorption.<sup>(13)</sup>

To reveal the mechanism of Ac45's role in osteoclastic bone resorption, we examined if Ac45-depleted osteoclasts impair lysosomal sorting and routing since V-ATPase recruitment to the ruffled border is a key step for acidification and bone resorption.<sup>(30,31)</sup> Instead of sorting toward the cell membrane, we found that lysosomes lost their targeted trafficking property and diffused throughout the cytoplasm in Ac45-depleted cells, as shown by the loss of V-ATPase polarization at the plasma membrane (Figs. 3B and 4). Use of osteoclasts as a polarized cell model in this study provides strong evidence that Ac45 is likely a regulator for lysosomal trafficking in a defined direction in osteoclasts and perhaps in other cells. This finding is consistent with a previous report that the cytoplasmic terminus of Ac45 contains autonomous targeting and sorting signals that contribute to the transport of the Ac45 protein in fibroblasts.<sup>(12)</sup> In osteoclasts, there are major implications for Ac45's role in lysosomal routing since V-ATPases must be recruited to the ruffled border in order to pump hydrogen ions into the resorptive lacuna, which creates a low pH microenvironment that contributes to bone resorption by degrading inorganic

**Fig. 4.** Depletion of Ac45 resulted in sorting failure and a loss of lysosomal trafficking to the ruffled border. (I) Three different antibodies anti-ATP6v0a3, anti-ATP6v1b2, and anti-ATP6v1c1 were used to localize V-ATPases either in (IA–I) nonresorptive cells on glass slices or (IJ–U) resorptive cells on dentin slices. Mock osteoclasts and osteoclasts transduced with Lentivirus-GFP-RNAi or Lentivirus-Ac45-RNAi(s1) after induction with M-CSF/RANKL for 48 hours were viewed as follows: (IA–I) Zeiss Axioplan microscope assay of V-ATPase localization; (IJ–R) horizontal views (x-y sections) of confocal microscopy analysis of V-ATPase localization; (Iz–Rz) lateral views (z-x sections) of cells stained for anti-ATP6v0a3, anti-ATP6v1b2, and anti-ATP6v1c1. The positions of confocal sections are shown by dotted lines in the corresponding images. (IS–U) Three-dimensional reconstruction of the cell on the bone surface. The length of the scale bar is 10  $\mu$ m. (II) Two different antibodies, anti-ATP6v0a3 (fluorescence appears green) and anti-lamp-1 (fluorescence appears red), were used to localize lysosomes in resorptive cells [mock osteoclasts and osteoclasts transduced with Lentivirus-GFP-RNAi or Lentivirus-Ac45-RNAi(s1)] on bone slices. (IIA–I) Three-dimensional reconstruction of cells on the bone surface. Nuclei were labeled using DAPI DNA stain, and appear blue in merged images. Yellow staining in merged images indicates colocalization of Atp6v0a3 and lamp-1. (IIJ–L) Slices and sections of IIG–I. The surface of the cells in xz and yz is outlined in white. The positions of confocal sections are shown by dotted lines in the corresponding images. White arrows indicate staining at the ruffled border. Blue arrows indicate staining in monocytes. The length of the scale bar is 20  $\mu$ m.

minerals.<sup>(32-34)</sup> Bone resorption also requires the secretion of proteolytic enzymes (eg, cathepsin K)<sup>(35,36)</sup> into the resorptive lacuna for organic matrix degradation. Our research revealed that cathepsin K exocytosis toward the resorption lacuna was remarkably reduced in Ac45-depleted osteoclasts (Fig. 5). Importantly, this appears to be specifically due to Ac45 deficiency, and not the general consequence of a defective V-ATPase, because ATP6v1e1 (an osteoclast V-ATPase subunit) depletion did not block cathepsin K exocytosis. Furthermore, the

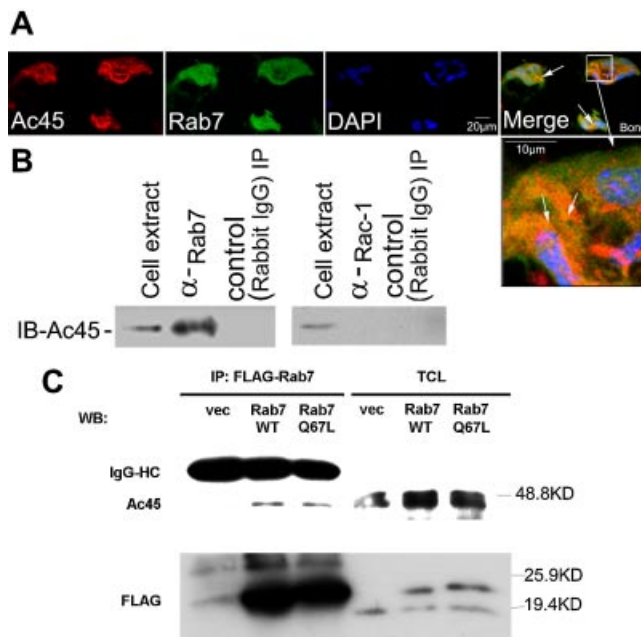
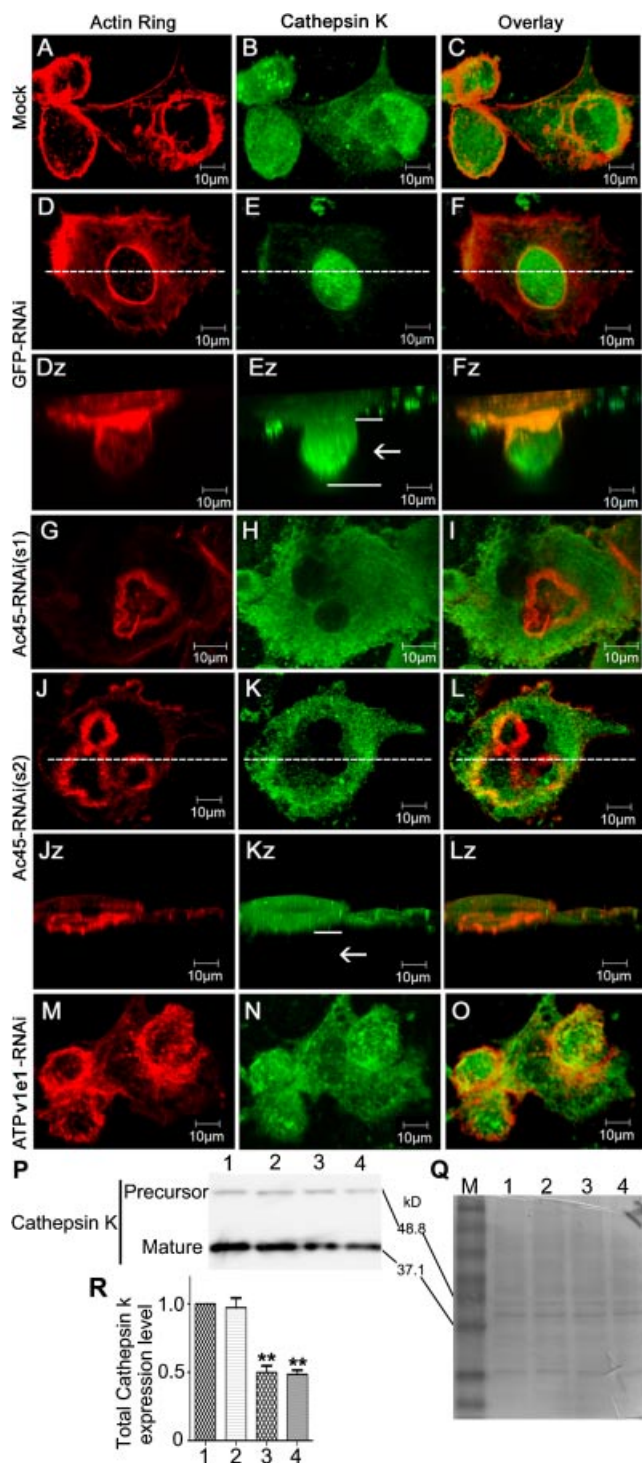


**Fig. 6.** Ac45 interacts with Rab7 in osteoclasts. (A) Ac45 colocalized with Rab7 (white arrows indicate colocalization) in resorbing osteoclasts cultured on bone slice. The cells shown are representative of the data. (B) Immunoblot of Ac45 when the whole-cell extracts were immunoprecipitated with anti-Rab7 and anti-Rac1. (C) Top left: Immunoprecipitation with anti-FLAG of cells transfected with recombinant viruses containing an empty vector as a control (vec), wild-type Rab7 (Rab7WT), and the active form of Rab7 (Rab7Q67L). The cells were analyzed by Western blot for the detection of Ac45 and IgG (positive control). Top right: Total cell lysates (TCL) of non-immunoprecipitated cells were analyzed with Western blot for Ac45 and IgG (negative control). Bottom: Immunoprecipitated cells and total cell lysates analyzed by Western blot for FLAG (control).

**Fig. 5.** Depletion of Ac45 causes defects in cathepsin K exocytosis. Cathepsin K was immunostained with anti-cathepsin K antibody and then co-stained with F-actin by secondary antibody conjugated with FITC and rhodamine phalloidin in (A–C) mock cells and osteoclasts transfected with (D–F, Dz–Fz) Lentivirus-GFP-RNAi, (G–I) Lentivirus-Ac45-RNAi(s1), (J–L, Jz–Lz) Lentivirus-Ac45-RNAi(s2), or (M–O) Lentivirus-ATP6v1e1-RNAi (as a control) after induction with M-CSF/RANKL for 48 hours. These resorbing cells were detected by confocal microscopy and analyzed by 3D reconstruction software Imaparis. Horizontal views (x-y sections) of 1- $\mu$ m thickness were taken 1  $\mu$ m above the bone surface. Lateral views (z-x sections) of (Dz–Fz) mock cells and (Jz–Lz) osteoclasts transfected with Lentivirus-Ac45-RNAi(s2) that were stained for the cathepsin K and actin. The lateral view reveals that unlike mock cells, osteoclasts transfected with Lentivirus-Ac45-RNAi(s2) do not form deep bone resorption pits as indicated by the white arrows and lines. The positions of confocal sections are shown by dotted lines in the corresponding images. The length of the scale bar is 10  $\mu$ m. (P) Representative Western blotting assay of cathepsin K protein level in osteoclast culture media as indicated. (Q) Representative ponceau S stain for Western blots of P. (R) Quantification of P (n = 3). In P–R, column 1 is mock, column 2 is Lentivirus-GFP-RNAi, column 3 is Lentivirus-Ac45-RNAi(s1), column 4 is Lentivirus-Ac45-RNAi(s2). In Q, M indicates marker. \*\*p < 0.01 compared with that of Lentivirus-GFP-RNAi treated cells. All results are mean  $\pm$  SD.

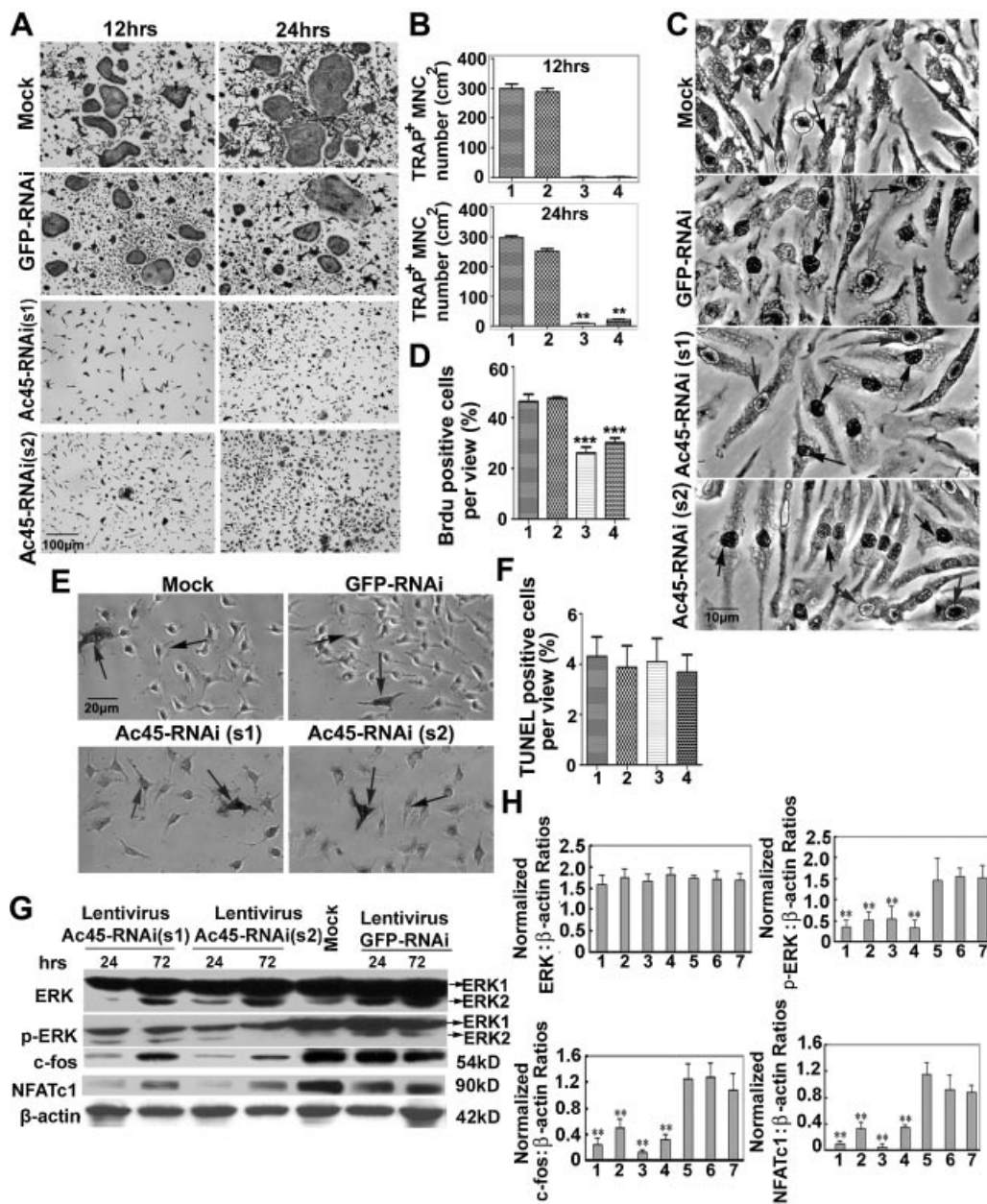


**Fig. 7.** Lentivirus-mediated knockdown of Ac45 impaired differentiation of mononuclear cells to mature osteoclasts, inhibited osteoclast precursor cell proliferation, and downregulated proteins that promote osteoclastogenesis, but had no effect on osteoclast precursor cell apoptosis. (A) TRAP staining of mock cells, as well as osteoclasts transduced with Lentivirus-GFP-RNAi, Lentivirus-Ac45-RNAi(s1), and Lentivirus-Ac45-RNAi(s2) after 12 or 24 hours of M-CSF/RANKL induction. (B) Quantification of TRAP<sup>+</sup> multinucleated cell (MNC) number ( $\geq 3$  nuclei) in A. All data are expressed as mean  $\pm$  SD ( $n = 5$ ). (C) Anti-BrdU staining of osteoclast precursor cells after 2.5 hours of incubation with BrdU and M-CSF. (Gray arrows indicate BrdU-positive cells and black arrows indicate BrdU-negative cells.) (D) Quantification of the percentage of BrdU-positive cells per view ( $n = 10$ ). (E) TUNEL staining of osteoclast precursor cells after 24 hours of incubation with media without FBS and M-CSF. (Gray arrows indicate TUNEL-positive cells and black arrows indicate TUNEL-negative cells.) (F) Quantification of the ratio of TUNEL-positive cells per view ( $n = 10$ ). In B, D, and F, column 1 is mock, column 2 is Lentivirus-GFP-RNAi, column 3 is Lentivirus-Ac45-RNAi(s1), and column 4 is Lentivirus-Ac45-RNAi(s2).  $**p < 0.01$ ,  $***p < 0.001$  compared with that of Lentivirus-GFP-RNAi-treated cells at the same time points of transduction. (G) Western blot analysis of expression levels of ERK, phosphorylated ERK (p-ERK), c-fos, and NFATc1 in mock osteoclasts and osteoclasts transduced by Lentivirus-GFP-RNAi (control), Lentivirus-Ac45-RNAi(s1), or Lentivirus-Ac45-RNAi(s2) after 24 or 72 hours of M-CSF/RANKL induction.  $\beta$ -actin was used as a protein loading control. (H) Quantification of the protein levels on blot (lanes 1–7). The values shown represent ratios of ERK, p-ERK, c-fos, or NFATc1 to  $\beta$ -actin protein levels that have been normalized ( $n = 3$ ).

function of cathepsin K exocytosis is independent from extracellular acidification because ATP6v1e1 knockdown resulted in impaired extracellular acidification (Fig. 3A), but maintained normal cathepsin K exocytosis (Fig. 5O). Our research indicates that defective lysosomal trafficking to the ruffled

border may partly contribute to the inhibited exocytosis of cathepsin K. However, it remains unknown to what degree the signaling pathways or biosynthetic vesicular trafficking routes that regulate these processes are similar or overlapping.<sup>(37)</sup> Importantly, we demonstrate for the first time that Ac45

regulates lysosomal trafficking and the exocytosis of cathepsin K, thereby affecting extracellular acidification and the important function of bone resorption.

Recent studies have shown that Ras GTPase-activating-like protein (IQGAP1) binds to cytoplasmic linker protein 170 (CLIP-170) and Rac1, which directly interacts with Rab7 and forms a complex that is capable of regulating the movement of acidic vesicles along microtubules to actin filaments and into the fusion zone of the ruffled border.<sup>(38)</sup> Indeed, inhibition of the expression of Rab7 impairs formation of the ruffled border and osteoclast secretion.<sup>(39)</sup> Notably, our research demonstrates that intracellular trafficking of lysosomes to the ruffled border is dramatically blocked when Ac45 is depleted (Fig. 4), indicating that Rab7 is not sufficient for vesicular trafficking in the absence of Ac45. As a transmembrane protein of vesicles and a protein which directly binds to Rab7, Ac45 has the potential to bridge the V-ATPase in vesicles to Rab7 and consequently drag the vesicle along the microtubule to the ruffled border. The potential role of Ac45 in vesicular trafficking is supported by our finding that Ac45 colocalizes with Rab7, and directly interacts with Rab7 (Fig. 6). Although detailed mechanisms of vesicular trafficking and cathepsin K exocytosis in osteoclasts remain to be elucidated, we suspect that the interaction of Ac45 with Rab7 may be involved in these processes. Based on our findings and the work of others,<sup>(38,40)</sup> we suggest that Ac45 may have the capacity to bridge the V-ATPase in vesicles to the Rab7-Rac1 complex and consequently drag the lysosome along the microtubule to the ruffled border.

Our study demonstrates for the first time that Ac45 has an important role in osteoclast differentiation through the ERK/c-fos/NFATc1 signaling pathway and in osteoclast-mediated protease exocytosis. We also demonstrate that Ac45 has an important role in the regulation of lysosomal trafficking to the ruffled border, possibly through a Rab7 signaling pathway. This research provides insight into the longstanding question of the mechanism underlying vesicular trafficking to the ruffled border and the related process of cathepsin K exocytosis. These findings suggest that Ac45 may be an ideal target for treating osteolytic diseases such as osteoporosis or rheumatoid arthritis.

## Disclosures

All authors state that they have no conflicts of interest.

## Acknowledgments

We express our deep gratitude to Dr. Weiguo Zou for his excellent help in the selection of siRNA. We also thank Dr. Lai Ding, Dr. Daniel Tom, and Dr. Shawn R Williams for their excellent technical assistance in confocal microscopy and three-dimensional reconstruction. We thank Dr. Peter V. Hauschka (Children's Hospital Boston) for providing us with dentin slices. This work was supported by NIH grants: AR-44741 (Y-PL) and AR-055307 (Y-PL), and by the Talents Training Program for Western China of China Scholarship Council.

Authors' roles: Study design: YPL. Study conduct: DQY, SF, WC, and HZ. Data collection: DQY, SF, and WC. Data analysis: DQY, SF,

and HZ. Data interpretation: DQY, SF, WC, CP, and YPL. Drafting manuscript: DQY and HZ. Revising manuscript content: SF, WC, CP, and YPL. Approving final version of manuscript: DQY, SF, WC, HZ, CP, and YPL. YPL takes responsibility for the integrity of the data analysis.

## References

1. Rousselle AV, Heymann D. Osteoclastic acidification pathways during bone resorption. *Bone*. 2002 Apr; 30(4):533–40.
2. Akisaka T, Yoshida H, Suzuki R, Takama K. Adhesion structures and their cytoskeleton-membrane interactions at podosomes of osteoclasts in culture. *Cell Tissue Res*. 2008 Mar; 331(3):625–41.
3. Palokangas H, Mulari M, Vaananen HK. Endocytic pathway from the basal plasma membrane to the ruffled border membrane in bone-resorbing osteoclasts. *J Cell Sci*. 1997 Aug; 110(Pt 15):1767–80.
4. Mulari MT, Zhao H, Lakkakorpi PT, Vaananen HK. Osteoclast ruffled border has distinct subdomains for secretion and degraded matrix uptake. *Traffic*. 2003 Feb; 4(2):113–25.
5. Mellman I, Nelson WJ. Coordinated protein sorting, targeting and distribution in polarized cells. *Nat Rev Mol Cell Biol*. 2008 Nov; 9(11):833–45.
6. Marshansky V, Futai M. The V-type H<sup>+</sup>-ATPase in vesicular trafficking: targeting, regulation and function. *Curr Opin Cell Biol*. 2008 Aug; 20(4):415–26.
7. Xu J, Cheng T, Feng HT, Pavlos NJ, Zheng MH. Structure and function of V-ATPases in osteoclasts: potential therapeutic targets for the treatment of osteolysis. *Histol Histopathol*. 2007 Apr; 22(4):443–54.
8. Wada Y, Sun-Wada GH, Tabata H, Kawamura N. Vacuolar-type proton ATPase as regulator of membrane dynamics in multicellular organisms. *J Bioenerg Biomembr*. 2008 Feb; 40(1):53–7.
9. Li YP, Chen W, Liang Y, Li E, Stashenko P. Atp6i-deficient mice exhibit severe osteopetrosis due to loss of osteoclast-mediated extracellular acidification. *Nat Genet*. 1999 Dec; 23(4):447–51.
10. Schoonderwoert VT, Martens GJ. Targeted disruption of the mouse gene encoding the V-ATPase accessory subunit Ac45. *Mol Membr Biol*. 2002 Jan; 19(1):67–71.
11. Louagie E, Taylor NA, Flamez D, Roebroek AJ, Bright NA, Meulemans S, Quintens R, Herrera PL, Schuit F, Van de Ven WJ, Creemers JW. Role of furin in granular acidification in the endocrine pancreas: identification of the V-ATPase subunit Ac45 as a candidate substrate. *Proc Natl Acad Sci U S A*. 2008 Aug 26; 105(34):12319–24.
12. Jansen EJ, Holthuis JC, McGrouther C, Burbach JP, Martens GJ. Intracellular trafficking of the vacuolar H<sup>+</sup>-ATPase accessory subunit Ac45. *J Cell Sci*. 1998 Oct; 111(Pt 20):2999–3006.
13. Feng H, Cheng T, Pavlos NJ, Yip KH, Carrello A, Seeber R, Eidne K, Zheng MH, Xu J. Cytoplasmic terminus of vacuolar type proton pump accessory subunit Ac45 is required for proper interaction with V(0) domain subunits and efficient osteoclastic bone resorption. *J Biol Chem*. 2008 May 9; 283(19):13194–204.
14. Schoonderwoert VT, Jansen EJ, Martens GJ. The fate of newly synthesized V-ATPase accessory subunit Ac45 in the secretory pathway. *Eur J Biochem*. 2002 Apr; 269(7):1844–53.
15. Feng S, Deng L, Chen W, Shao J, Xu G, Li YP. Atp6v1c1 is an essential component of the osteoclast proton pump and in F-actin ring formation in osteoclasts. *Biochem J*. 2009 Jan 1; 417(1):195–203.
16. Wu H, Xu G, Li YP. Atp6v0d2 is an essential component of the osteoclast-specific proton pump that mediates extracellular acidification in bone resorption. *J Bone Miner Res*. 2009 May; 24(5):871–85.
17. Henshall SM, Afar DE, Hiller J, Horvath LG, Quinn DI, Rasiyah KK, Gish K, Willhite D, Kench JG, Gardiner-Garden M, Stricker PD, Scher HI, Grygiel JJ, Agus DB, Mack DH, Sutherland RL. Survival analysis of genome-wide gene expression profiles of prostate cancers identifies

- new prognostic targets of disease relapse. *Cancer Res.* 2003 Jul 15; 63(14):4196–203.
18. Kim K, Lee SH, Ha KJ, Choi Y, Kim N. NFATc1 induces osteoclast fusion via up-regulation of Atp6v0d2 and the dendritic cell-specific transmembrane protein (DC-STAMP). *Mol Endocrinol.* 2008 Jan; 22(1): 176–85.
  19. Yagi M, Miyamoto T, Sawatani Y, Iwamoto K, Hosogane N, Fujita N, Morita K, Ninomiya K, Suzuki T, Miyamoto K, Oike Y, Takeya M, Toyama Y, Suda T. DC-STAMP is essential for cell-cell fusion in osteoclasts and foreign body giant cells. *J Exp Med.* 2005 Aug 1; 202(3):345–51.
  20. Blair HC, Teitelbaum SL, Ghiselli R, Gluck S. Osteoclastic bone resorption by a polarized vacuolar proton pump. *Science.* 1989 Aug 25; 245(4920):855–7.
  21. Baron R, Neff L, Louvard D, Courtoy PJ. Cell-mediated extracellular acidification and bone resorption: evidence for a low pH in resorbing lacunae and localization of a 100-kD lysosomal membrane protein at the osteoclast ruffled border. *J Cell Biol.* 1985;101:2210–22.
  22. Dechant R, Binda M, Lee SS, Pelet S, Winderickx J, Peter M. Cytosolic pH is a second messenger for glucose and regulates the PKA pathway through V-ATPase. *EMBO J.* 2010 Aug 4; 29(15):2515–26.
  23. Toyomura T, Murata Y, Yamamoto A, Oka T, Sun-Wada GH, Wada Y, Futai M. From lysosomes to the plasma membrane: localization of vacuolar-type H<sup>+</sup>-ATPase with the a3 isoform during osteoclast differentiation. *J Biol Chem.* 2003 Jun 13; 278(24): 22023–30.
  24. van Hille B, Richener H, Schmid P, Puettner I, Green JR, Bille G. Heterogeneity of vacuolar H<sup>+</sup>-ATPase: differential expression of two human subunit B isoforms. *Biochem J.* 1994 Oct 1; 303(Pt 1): 191–8.
  25. Zhao H, Ettala O, Vaananen HK. Intracellular membrane trafficking pathways in bone-resorbing osteoclasts revealed by cloning and subcellular localization studies of small GTP-binding rab proteins. *Biochem Biophys Res Commun.* 2002 May 10; 293(3): 1060–5.
  26. Takayanagi H, Kim S, Koga T, Nishina H, Isshiki M, Yoshida H, Saiura A, Isobe M, Yokochi T, Inoue J, Wagner EF, Mak TW, Kodama T, Taniguchi T. Induction and activation of the transcription factor NFATc1 (NFAT2) integrate RANKL signaling in terminal differentiation of osteoclasts. *Dev Cell.* 2002 Dec; 3(6):889–901.
  27. Qin A, Cheng TS, Lin Z, Pavlos NJ, Jiang Q, Xu J, Dai KR, Zheng MH. Versatile roles of V-ATPases accessory subunit Ac45 in osteoclast formation and function. *PLoS One.* 2011;6(11):e27155.
  28. Soltanoff CS, Yang S, Chen W, Li YP. Signaling networks that control the lineage commitment and differentiation of bone cells. *Crit Rev Eukaryot Gene Expr.* 2009;19(1):1–46.
  29. Murphy LO, Blenis J. MAPK signal specificity: the right place at the right time. *Trends Biochem Sci.* 2006 May; 31(5):268–75.
  30. Vaananen HK, Karhukorpi EK, Sundquist K, Wallmark B, Roininen I, Hentunen T, Tuukkanen J, Lakkakorpi P. Evidence for the presence of a proton pump of the vacuolar H<sup>+</sup>-ATPase type in the ruffled borders of osteoclasts. *J Cell Biol.* 1990 Sep; 111(3):1305–11.
  31. Mulari M, Vaaraniemi J, Vaananen HK. Intracellular membrane trafficking in bone resorbing osteoclasts. *Microsc Res Tech.* 2003 Aug 15; 61(6):496–503.
  32. Teitelbaum SL. Bone resorption by osteoclasts. *Science.* 2000 Sep 1; 289(5484):1504–8.
  33. Teitelbaum SL, Ross FP. Genetic regulation of osteoclast development and function. *Nat Rev Genet.* 2003 Aug; 4(8):638–49.
  34. Vaananen HK, Zhao H, Mulari M, Halleen JM. The cell biology of osteoclast function. *J Cell Sci.* 2000 Feb; 113(Pt 3):377–81.
  35. Saftig P, Hunziker E, Wehmeyer O, Jones S, Boyde A, Rommerskirch W, Moritz JD, Schu P, von Figura K. Impaired osteoclastic bone resorption leads to osteopetrosis in cathepsin-K-deficient mice. *Proc Natl Acad Sci U S A.* 1998 Nov 10; 95(23):13453–8.
  36. Gelb BD, Shi GP, Chapman HA, Desnick RJ. Pycnodysostosis, a lysosomal disease caused by cathepsin K deficiency. *Science.* 1996 Aug 30; 273(5279):1236–8.
  37. Coxon FP, Taylor A. Vesicular trafficking in osteoclasts. *Semin Cell Dev Biol.* 2008 Oct; 19(5):424–33.
  38. Sun Y, Buki KG, Ettala O, Vaaraniemi JP, Vaananen HK. Possible role of direct Rac1-Rab7 interaction in ruffled border formation of osteoclasts. *J Biol Chem.* 2005 Sep 16; 280(37):32356–61.
  39. Zhao H, Laitala-Leinonen T, Parikka V, Vaananen HK. Downregulation of small GTPase Rab7 impairs osteoclast polarization and bone resorption. *J Biol Chem.* 2001 Oct 19; 276(42):39295–302.
  40. Vitavska O, Merzendorfer H, Wiczorek H. The V-ATPase subunit C binds to polymeric F-actin as well as to monomeric G-actin and induces cross-linking of actin filaments. *J Biol Chem.* 2005 Jan 14; 280(2):1070–6.